Reentrant phase transitions of quantum black holes

Antonia M. Frassino,[1,2] Juan F. Pedraza,[3] Andrew Svesko,[4,5] and Manus R. Visser[6]

[1]*Departamento de Física y Matemáticas, University of Alcalá, Campus universitario 28805, Alcalá de Henares (Madrid), Spain*

[2]*Departament de Física Quàntica i Astrofísica and Institut de Ciències del Cosmos, Universitat de Barcelona, Barcelona 08028, Spain*

[3]*Instituto de Física Teórica UAM/CSIC Calle Nicolás Cabrera 13-15, Cantoblanco, Madrid 28049, Spain*

[4]*Department of Physics and Astronomy, University College London, London WC1E 6BT, United Kingdom*

[5]*Department of Mathematics, King's College London, Strand, London WC2R 2LS, United Kingdom*

[6]*Department of Applied Mathematics and Theoretical Physics, University of Cambridge, Cambridge CB3 0WA, United Kingdom*

(Received 9 November 2023; accepted 9 May 2024; published 14 June 2024)

We show that backreaction of quantum fields on black hole geometries can trigger new thermal phase transitions. Specifically, we study the phase behavior of the three-dimensional quantum-corrected static Bañados-Teitelboim-Zanelli black hole, an exact solution to specific semiclassical gravitational equations due to quantum conformal matter, discovered through braneworld holography. Focusing on the canonical ensemble, for large backreaction, we find novel reentrant phase transitions as the temperature monotonically increases, namely, from thermal anti–de Sitter space to the black hole and back to thermal anti–de Sitter. The former phase transition is first-order, a quantum analog of the classical Hawking-Page phase transition, while the latter is zeroth order and has no classical counterpart.

DOI: 10.1103/PhysRevD.109.124040

I. INTRODUCTION

Black hole thermodynamics offers a window into the nature of quantum gravity. A paradigmatic example is the Hawking-Page (HP) phase transition of black holes in asymptotically anti–de Sitter (AdS) space [1]; below a certain temperature, large AdS black holes in equilibrium with radiation give way to thermal AdS, signaling an exchange of the dominant contribution to the quantum gravitational partition function. Originally discovered for four-dimensional Schwarzschild-AdS black holes, the HP transition also exists for their three-dimensional counterparts [2–5], i.e., Bañados-Teitelboim-Zanelli (BTZ) black holes [6,7]. To wit, a static BTZ black hole of mass M has metric,

$$ds^2 = -f(r)dt^2 + \frac{dr^2}{f(r)} + r^2 d\phi^2,$$
$$f(r) = \frac{r^2}{\ell_3^2} - 8G_3 M, \tag{1}$$

with AdS_3 length scale ℓ_3, three-dimensional Newton's constant G_3, and has horizon radius $r_+^2 = 8G_3 M\ell_3^2$. Via the canonical partition function, the BTZ free energy is

$$F_{\rm BTZ} = M - TS = -\frac{\pi^2\ell_3^2}{2G_3}T^2, \tag{2}$$

for temperature $T = r_+/2\pi\ell_3^2$ and entropy $S = 2\pi r_+/4G_3$. Comparing to the free energy of thermal AdS, $F_{\rm AdS} = M_{\rm AdS} = -1/8G_3$, a first-order phase transition occurs at a temperature $T_{\rm HP} = 1/(2\pi\ell_3)$. When $T < T_{\rm HP}$, thermal AdS has a lower free energy than the black hole, while for $T > T_{\rm HP}$ the black hole becomes the dominant contribution to the partition function.

The study of such gravitational phase transitions has expanded to a plethora of black hole backgrounds, revealing rich physical phenomena. For instance, Reissner-Nordström AdS black holes undergo a first-order phase transition between large and small black holes analogous to the liquid/gas phase change of van der Waals fluids [8–10], displaying the same critical behavior [11]. Moreover, reentrant phase transitions—a sequence of two or more phase transitions due to a monotonic change to any thermal quantity where the initial and final states are macroscopically similar—occur for, e.g., $d = 4$ Born-Infeld AdS black holes [12], rotating AdS black holes in $d \geq 6$ dimensions [13,14], or $U(1)$ charged Lovelock black holes [15], sharing traits akin to multicomponent fluids, binary gases, and liquid crystals [16].

Each of these studies consider classical black hole backgrounds. It is natural to wonder how quantum matter

influences black hole phase transitions through semiclassical backreaction. A complete treatment of this question, however, requires solving the semiclassical Einstein equations, $G_{ab} = 8\pi G\langle T_{ab}\rangle$, a difficult and open problem in higher than two spacetime dimensions.

Here we use braneworld holography [17] to exactly study phase transitions of semiclassical black holes to all orders of backreaction due to a large number of quantum fields. In this framework a d-dimensional end-of-the-world brane is coupled to Einstein's general relativity in an asymptotically $(d+1)$-dimensional AdS background, which has a dual holographic interpretation as a conformal field theory (CFT) living on the AdS boundary. In effect, the brane, typically located a small distance away from the AdS boundary, renders the (on shell) bulk action finite by integrating out bulk degrees of freedom up to the brane, as in holographic regularization [18]. This procedure induces a specific higher curvature gravity theory on the brane, coupled to a CFT with an ultraviolet cutoff that backreacts on the dynamical brane geometry. Thence, classical solutions to the bulk Einstein equations exactly correspond to solutions of the semiclassical field equations on the brane. Specifically, classical AdS black holes map to quantum-corrected black holes on the brane, to all orders of backreaction [19].

II. QUANTUM BTZ BLACK HOLE

We will study the phase transitions of a specific braneworld model, the three-dimensional quantum BTZ (qBTZ) family of black holes [20]. This solution follows from introducing an AdS_3 brane [21] inside a static, asymptotically AdS_4 geometry described by the C-metric [20,22,23]. The brane intersects the AdS_4 black hole horizon such that the horizon localizes on the brane. Via braneworld holography, the backreacted geometry and horizon thermodynamics of the qBTZ are known analytically, allowing for an exact description of its phase structure.

The metric of the quantum BTZ black hole is [20]

$$ds^2 = -f(r)dt^2 + \frac{dr^2}{f(r)} + r^2 d\phi^2,$$
$$f(r) = \frac{r^2}{\ell_3^2} - 8\mathcal{G}_3 M - \frac{\ell\mathcal{F}(M)}{r}, \tag{3}$$

with horizon radius r_+ being the largest root of $f(r_+) = 0$. Here M is the mass, ℓ represents an infrared bulk cutoff length, and $\mathcal{G}_3 = G_3/\sqrt{1+(\ell/\ell_3)^2}$ is the "renormalized" Newton's constant. Note for $\ell = 0$ the classical BTZ metric (1) is recovered. The form function $\mathcal{F}(M)$ is found by solving the brane equations of motion [20]

$$\mathcal{F}(M) = 8\frac{1-\kappa x_1^2}{(3-\kappa x_1^2)^3}, \tag{4}$$

where $\kappa = \pm 1, 0$ corresponds to different brane slicings ($\kappa = -1$ gives a BTZ black hole) and x_1 is a parameter controlling the mass, see Eq. (7). Together, (x_1, κ) parametrize a family of brane black holes and black strings covering a finite range of masses [22,23]. Classically, these solutions exist in disconnected branches of allowed masses, while quantum effects unify these branches. Lastly, the AdS_3 radius ℓ_3 is related to the (induced) brane cosmological constant,

$$\Lambda_3 \equiv -\frac{1}{L_3^2} = -2\left(\frac{1}{\ell^2} + \frac{1}{\ell_3^2} - \frac{1}{\ell}\sqrt{\frac{1}{\ell^2} + \frac{1}{\ell_3^2}}\right). \tag{5}$$

The metric (3) can be understood as a "quantum" black hole in the sense it is guaranteed to be a solution to the full semiclassical theory on the brane at all orders in quantum backreaction. The parameter ℓ controls the strength of the backreaction due to the CFT_3, and also features in the central charge c_3 of the cutoff CFT_3 [20]

$$c_3 = \frac{\ell}{2G_3\sqrt{1+(\ell/\ell_3)^2}}. \tag{6}$$

For a small backreaction, $\ell/\ell_3 \ll 1$, then $L_3^2 \approx \ell_3^2$ while $2c_3G_3 \approx \ell$. Thus, for fixed c_3, gravity becomes weak on the brane as $\ell \to 0$ such that there is no backreaction due to the CFT and no renormalization of Newton's constant. Lastly, note $\ell \approx 2c_3 L_P$, where $L_P = G_3$ is the three-dimensional Planck length (with $\hbar = 1$). Hence, the quantum correction in the qBTZ metric is not a Planckian effect since $c_3 \gg 1$.

III. THERMODYNAMICS OF THE QUANTUM BTZ BLACK HOLE

The thermodynamics of the quantum BTZ black hole on the brane is inherited from the black hole thermodynamics in the bulk. The AdS_4 C-metric describes an accelerating black hole, however, there is no acceleration horizon in our setup since we work in the regime of "small acceleration" [24]. Hence, there is only a black hole horizon in thermal equilibrium with its surrounding. The mass M, temperature T and entropy S of the classical bulk black hole are [20,23] (see also [25])

$$M = \frac{\sqrt{1+\nu^2}}{2G_3}\frac{z^2(1-\nu z^3)(1+\nu z)}{(1+3z^2+2\nu z^3)^2}, \tag{7}$$

$$T = \frac{1}{2\pi\ell_3}\frac{z(2+3\nu z+\nu z^3)}{1+3z^2+2\nu z^3}, \tag{8}$$

$$S = \frac{\pi\ell_3\sqrt{1+\nu^2}}{G_3}\frac{z}{1+3z^2+2\nu z^3}, \tag{9}$$

where $z \equiv \ell_3/(r_+x_1)$ and $\nu \equiv \ell/\ell_3$ both have range $[0,\infty)$. Each quantity may be derived by identifying the bulk on

shell Euclidean action with the canonical free energy [25]. Previous work [24,26] examined accelerating black hole thermodynamics but not in the presence of a brane.

From the brane perspective, the qBTZ black hole has the same temperature T, while the four-dimensional Bekenstein-Hawking entropy S is identified with the three-dimensional generalized entropy, $S \equiv S_{\rm gen}$ [20,27], accounting for both higher-curvature corrections and semiclassical matter effects. Thus, if ℓ and ℓ_3 are kept fixed, the qBTZ first law takes the standard form,

$$dM = T dS_{\rm gen}, \tag{10}$$

valid to all orders in backreaction, and where the qBTZ mass is identified as M. Classical entropy being replaced by the generalized entropy in the first law also occurs for two-dimensional semiclassical black holes [28,29].

The thermal quantities obey the Smarr relation [30],

$$0 = TS_{\rm gen} - 2P_3V_3 + \mu_3 c_3, \tag{11}$$

where $P_3 = -\Lambda_3/(8\pi G_3)$ is the pressure with conjugate "thermodynamic volume" V_3, and μ_3 is the chemical potential conjugate to c_3 (see Ref. [30] for exact expressions in terms of ℓ_3, z and ν). Unlike higher-dimensional Smarr formulas, the mass is absent from the three-dimensional Smarr relation (11) since G_3M has vanishing scaling dimension, as with the classical BTZ black hole [31,32].

The appearance of extra thermodynamic variables in the Smarr relation (11) suggests an extended black hole thermodynamics [33]. Specifically, the first law (10) generalizes to include pressure and central charge variations

$$dM = T dS_{\rm gen} + V_3 dP_3 + \mu_3 dc_3. \tag{12}$$

In the context of braneworld holography, extended thermodynamics of black holes on the brane is naturally induced from the standard thermodynamics of bulk black holes including work done by the brane, e.g., dynamical pressure P_3 corresponds to variable brane tension [30]. Here, however, we focus on the canonical ensemble, defined by fixing (T, P_3, c_3).

In Fig. 1 we plot temperature as a function of z at fixed P_3 and c_3. For all pressure—except a critical one $P_3 = P_{\rm crit}$—the temperature has two turning points, signifying three branches: (A) "cold" black hole, $z \in (0, z_{\rm max})$, with $z_{\rm max}$ denoting the local maximum of T; (B) "intermediate" black hole, $z \in (z_{\rm max}, z_{\rm min})$, with $z_{\rm min}$ marking the local minimum of T, and (C) "hot" black hole, $z \in (z_{\rm min}, \infty)$. (This terminology is motivated by the end behavior of $T(z)$, but, note that branch B black holes can have temperatures less than those in branch A.) For $\nu > 1$, $z_{\rm max} = \nu^{-1/3}$ and $z_{\rm min}$ is the positive root of $\nu z^3 + 3z^2 - 3\nu z - 1 = 0$, and conversely, for $\nu < 1$, $z_{\rm min} = \nu^{-1/3}$ while $z_{\rm max}$ is the positive root of the same equation;

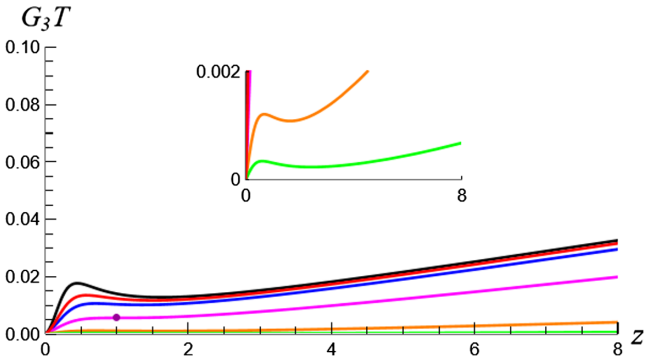

FIG. 1. Temperature of qBTZ black hole at $c_3 = 10$ and various pressures (from bottom to top): $G_3^3P_3 = \{5.0 \times 10^{-7}\,(\text{green}), 5.0 \times 10^{-6}\,(\text{orange}), G_3^3P_{\rm crit} \approx 5.83 \times 10^{-5}\,(\text{magenta}), 1.33 \times 10^{-4}\,(\text{blue}), 1.61 \times 10^{-4}\,(\text{red}), 1.81 \times 10^{-4}\,(\text{black})\}$. The critical line inflection point is in purple.

for any ν, $z_{\rm max} < z_{\rm min}$, except when $\nu = 1$, where $z_{\rm max} = z_{\rm min} = z_{\rm crit}$ (see below). Notably, for $\nu > 1$, branch A typifies black holes with masses $0 < M < 1/24\mathcal{G}_3$, while B and C branches have $-1/8\mathcal{G}_3 < M < 0$ (with $M = 0$ at $z = 0, z_{\rm max}$). Alternately, for $\nu < 1$, branches A and B have $0 < M < 1/24\mathcal{G}_3$, and branch C has $-1/8\mathcal{G}_3 < M < 0$ (with $M = 0$ at $z = 0, z_{\rm min}$) [34]. In contrast, classical BTZ has a single branch of black holes since T is monotonic in r_+.

Further, for qBTZ the temperature has an inflection point when both the first and second z-derivatives of T at fixed ν vanish. This occurs when $z_{\rm crit} = \nu_{\rm crit} = 1$ and yields the following critical pressure and temperature

$$P_{\rm crit} = \frac{1}{16\pi c_3^2 G_3^3 (2+\sqrt{2})}, \qquad T_{\rm crit} = \frac{1}{4\sqrt{2}\pi c_3 G_3}. \tag{13}$$

Both expressions depend on the fixed central charge. Alternately, we can fix the pressure, yielding the critical central charge given by the inverse of (13), $c_{\rm crit} \propto 1/\sqrt{P_3}$.

IV. PHASE TRANSITIONS OF THE QUANTUM BTZ BLACK HOLE

We focus on thermal phase behavior of the quantum BTZ black hole in the canonical ensemble with free energy

$$\begin{aligned} F_{\rm qBTZ} &\equiv M - TS_{\rm gen} \\ &= -\frac{z^2\sqrt{1+\nu^2}}{2G_3}\frac{[1+2\nu z+\nu z^3(2+\nu z)]}{(1+3z^2+2\nu z^3)^2}. \end{aligned} \tag{14}$$

Here we expressed the free energy in terms of ν, but we can use (5) and (6) to rewrite ν in terms of P_3 and c_3,

$$\nu = \frac{\sqrt{32\pi c_3^2 G_3^3 P_3 (1 - 8\pi c_3^2 G_3^3 P_3)}}{1 - 16\pi c_3^2 G_3^3 P_3}. \tag{15}$$

Observe ν diverges when $c_3^2 G_3^2 P_3 = 1/16\pi$, placing an upper bound on pressure, $P_3 < 1/16\pi c_3^2 G_3^3$. Also note the canonical ensemble is equivalent to a fixed ν ensemble.

Analogous to the classical case [1], the qBTZ black hole can transition into thermal AdS, since at fixed pressure and central charge the black hole can evaporate due to Hawking radiation, and, conversely, thermal AdS can transition into a qBTZ black hole via collapse of the thermal gas. Thus, to analyze the phase behavior, we compare the free energy of the qBTZ black hole to that of "quantum" thermal AdS_3 (qTAdS) geometry, i.e., pure AdS_3 including backreaction due to the cutoff CFT_3 on the brane. This geometry contains thermal radiation in equilibrium at an arbitrary temperature since the CFT_3 is taken to be in a thermal state. Explicitly, the qTAdS geometry takes the form (3), with $\mathcal{F}(M) = 0$ and $M_{\mathrm{qTAdS}} = -1/8\mathcal{G}_3$, coinciding with the $z \to \infty$ limit of the qBTZ solution. Notice that while backreaction does not alter the form of the metric from classical AdS_3, the CFT_3 makes itself felt through the parameter ν in $\mathcal{G}_3$. Thus, the sole effect of backreaction due to conformal matter in thermal AdS_3 is to renormalize Newton's constant. An analogous result occurs for semiclassical Jackiw-Teitelboim gravity; backreaction due to conformal matter does not break the symmetries of the AdS_2 geometry, only the dilaton (or, equivalently, the effective two-dimensional Newton constant) receives quantum corrections (e.g., [28]). Further, in this limit the generalized entropy (9) vanishes, a consequence of quantum fluctuations renormalizing G_3 (capturing the spirit of [35]), and the free energy (14) becomes $F_{\mathrm{qTAdS}} = M_{\mathrm{qTAdS}} = -1/8\mathcal{G}_3$.

In Fig. 2 we make a parametric plot of the free energy difference $\Delta F \equiv F_{\mathrm{qBTZ}} - F_{\mathrm{qTAdS}}$ versus temperature T (using z as the parameter). At $P = P_{\mathrm{crit}}$ the free energy plot is smooth. However, for all positive values $P \neq P_{\mathrm{crit}}$ the free energy diagram shows inverse swallowtail behavior and contains three different branches; cold, intermediate and hot black hole branches, corresponding to the branches in Fig. 1. The cold branch begins at small temperature and ends at the lower-right cusp ($z = z_{\mathrm{max}}$), whereas the hot branch corresponds to the "horizontal" line that extends from the upper-left cusp ($z = z_{\mathrm{min}}$) off to high temperature. The intermediate branch is the curve connecting these two cusps. Since the free energy F_{qBTZ} and temperature go to zero as $z \to 0$, the difference ΔF does not vanish at zero temperature; instead it starts from a positive value that depends on P_3 and c_3.

The free energy plot displays phase transitions between thermal AdS and the qBTZ black hole for a certain pressure and temperature range. Since we are subtracting the free energy of thermal AdS, the black hole branches below the horizontal axis of the plot in Fig. 2 are the only ones that are thermodynamically favored with respect to thermal AdS. Everywhere else, thermal AdS has a lower free energy than the black hole. When the right cusp intersects $\Delta F = 0$, that is the starting point of the phase transitions. The

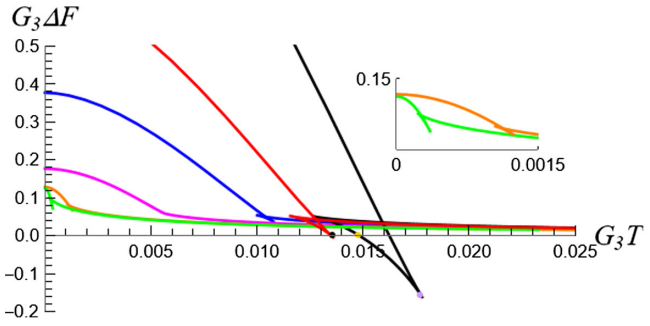

FIG. 2. Free energy difference of the qBTZ black hole and quantum thermal AdS at $c_3 = 10$ and various pressures P_3 (same values as in Fig. 1, ordered left to right). For $P_3 \neq P_{\mathrm{crit}}$ the free energy as a function of the temperature has inverse swallowtail behavior and consists of three branches. For small pressures, thermal AdS (with $\Delta F = 0$) always dominates. For $G_3^3 P_3 > 1.6135 \times 10^{-4}$ (red, center curve), thermal AdS dominates for small and large temperatures, and in between the intermediate branch has the lowest free energy. A first-order phase transition between thermal AdS and the intermediate branch occurs if this branch intersects the $\Delta F = 0$ line (yellow point), and a zeroth-order phase transition occurs at the right cusp (purple point). The phase transitions coincide when the right cusp intersects $\Delta F = 0$ (black point).

temperature and pressure where this occurs are found by solving when $\Delta F = 0$ and $z = z_{\mathrm{max}}$, at $\nu = 3\sqrt{3}$ and $z = 1/\sqrt{3}$, giving

$$T_0 = \frac{\sqrt{3}}{2\pi\ell_3} = \frac{9}{8\sqrt{7}\pi c_3 G_3}, \qquad P_0 = \frac{14-\sqrt{7}}{224\pi c_3^2 G_3^3}. \tag{16}$$

Note T_0 is larger than the classical HP temperature.

For larger pressures, as the temperature monotonically increases, there are *reentrant phase transitions* from thermal AdS to qBTZ and back to thermal AdS. The former transition occurs when branch B intersects the $\Delta F = 0$ line. Since there is a discontinuity in the slope of the free energy, this is a first-order phase transition, a quantum analog of the Hawking-Page phase transition. The latter transition between the branch B of qBTZ and thermal AdS occurs at the right cusp. Since there is a jump discontinuity in the free energy, this is a zeroth-order phase transition. Thus, the reentrant phase transition is described by the combination of the first- and zeroth-order phase transitions as the temperature monotonically varies. In the P_3 vs T phase diagram at fixed c_3 (Fig. 3) we depict coexistence lines of first- and zeroth-order phase transitions. The (black) intersection point of the two phase transitions (16) is neither representative of a second-order phase transition or a critical point.

Notably, such reentrant phase transitions do not occur for the classical BTZ black hole. As noted, here the zeroth-order phase transitions only occur for large enough P_3, or, correspondingly, $\nu > 3\sqrt{3}$, i.e., large backreaction. In this

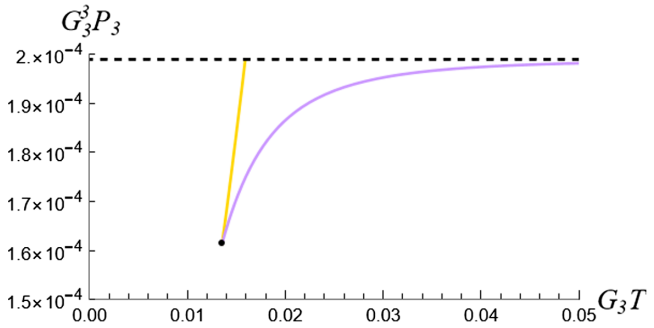

FIG. 3. P_3 versus T phase diagram at fixed $c_3 = 10$. The dashed black line corresponds to $\nu \to \infty$. The straight yellow and curved purple lines denote lines of first- and zeroth-order phase transitions, respectively. In the region between the yellow and purple curves the qBTZ black hole is thermally favored; thermal AdS dominates the canonical ensemble outside this region. The (black) cusp where the yellow and purple lines meet corresponds to $G_3^3P_0 = 1.6135 \times 10^{-4}$ and $G_3T_0 = 0.0135$. The isolated critical point lies at $G_3^3P_{\rm crit} \approx 5.83 \times 10^{-5}$ and $G_3T_{\rm crit} \approx 5.63 \times 10^{-3}$ (not shown).

regime, the brane has decreasing tension and the gravitational theory on the brane becomes more massive and effectively four dimensional [20].

The heat capacity allows us to determine which branches are stable under thermal fluctuations [25],

$$C_{P_3,c_3} = T\left(\frac{\partial S_{\rm gen}}{\partial T}\right)_{P_3,c_3} = \frac{\sqrt{1+\nu^2}\pi\ell_3}{2G_3(1-\nu z^3)}\frac{z(2+3\nu z+\nu z^3)(3z^2-1+4\nu z^3)}{(3z^2-1-3\nu z+\nu z^3)(1+3z^2+2\nu z^3)}. \tag{17}$$

In Fig. 4 we plot the heat capacity (17) versus temperature at fixed P_3 and c_3. For $T \neq T_{\rm crit}$ the cold black hole branch has partly positive and negative heat capacity, while the intermediate branch has $C_{P_3,c_3} > 0$ and the hot branch has $C_{P_3,c_3} < 0$. The heat capacity vanishes for a z_1 that is the positive root of $4z^3\nu + 3z^2 - 1 = 0$ (for $\nu \neq 1$), and diverges at $z_{\rm min}$ and $z_{\rm max}$, where $z_1 < z_{\rm max} < z_{\rm min}$. Note that the quantum Hawking-Page transition is between qTAdS and a "stable" black hole branch, as in the classical HP transition.

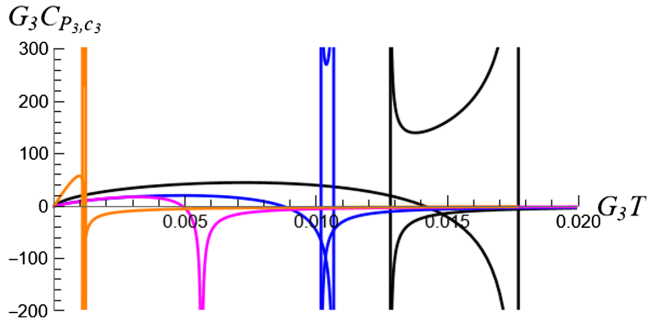

FIG. 4. Heat capacity at fixed pressure and central charge for select parameters in Fig. 1 [from left to right: 5.0×10^{-6} (orange), $G_3^3P_{\rm crit} \approx 5.83 \times 10^{-5}$ (magenta), 1.33×10^{-4} (blue), 1.81×10^{-4} (black)].

V. DISCUSSION

We used braneworld holography to study the thermal phase structure of black holes corrected due to semiclassical backreaction. Aside from a quantum counterpart of the first-order Hawking-Page transition, the qBTZ black hole also undergoes zeroth order phase transitions—a feature solely due to semiclassical effects. The physical viability of the zeroth-order phase transition is questionable, since such transitions typically do not occur in nature, for thermodynamically stable systems. A zeroth-order phase transition may be indicating we are missing a novel phase with lower free energy. For instance, the black hole could transition into a system with additional degrees of freedom or "hair" that are not captured by the qBTZ solution. We leave this for future investigation.

The free energy of the braneworld black holes investigated here was previously derived in [25] from the four-dimensional bulk perspective, however, that analysis lacked a physical interpretation in terms of quantum black holes and reentrant phase transitions were not observed. Our analysis on the brane carries over to the bulk and thus suggests this is the first example of a semiclassical black hole undergoing such a thermal reentrant phase transition. Further, we emphasize that the type of reentrant phase transition we uncover differs from those which have appeared in previous literature [12–15], which describe transitions between different phases of the black hole, e.g., from large to small and back to large black holes. Meanwhile, the reentrant phase transition we find is from thermal AdS to the black hole and back to thermal AdS, i.e., a reentrant Hawking-Page phase transition. Notably, only for large backreaction do the reentrant phase transitions occur. This suggests such features are unlikely to be found via standard perturbative techniques in studying quantum backreaction [36–38].

Since the brane geometry is asymptotically AdS, the brane gravity theory has a holographic interpretation in terms of a two-dimensional (defect) CFT, where all $1/c$ corrections are accounted for in a large central charge-c expansion. Thus, via this second layer of AdS/CFT duality, the phase transitions of the qBTZ black hole should have a dual interpretation [30]. Classically, the HP phase transition is argued to be dual to the (de)confinement transition of a large-c conformal gauge theory [39]. Our analysis implies the phase structure of the thermal $\rm CFT_2$ dual to the qBTZ black hole drastically changes when including all $1/c$ effects. Namely, in the canonical ensemble the temperature of the first-order phase transition changes and a new

zeroth-order phase transition arises, leading to reentrant transitions between (de)confined phases. It would be worth studying these new features from a microscopic perspective [40]. The bulk and brane system, moreover, is dual to a boundary CFT_3 ($BCFT_3$) [41,42]. Since the qBTZ free energy is equal to the bulk black hole free energy, thus having the same phase behavior, the dual $BCFT_3$ should exhibit reentrant phase transitions. It would be interesting to study this further.

Our study offers many future explorations. Firstly, we focused on the canonical ensemble. In fact, the static qBTZ black hole has four different ensembles (at fixed temperature) to examine. A study of ensembles at fixed thermodynamic volume (initiated in [43]) will shed new light on the instability of "superentropic" black holes [44,45], its microscopic interpretation [46], along with other inequalities constraining (extended) thermodynamic variables [47,48]. Further, our analysis can be generalized to other quantum black holes, e.g., rotating and charged qBTZ [20,49], or quantum de Sitter black holes [50,51]. Adding rotation or charge will enrich the phase structure. Lastly, we focused on black holes in three dimensions. It is natural to wonder how to generalize to higher dimensions. So far finding higher-dimensional braneworld black holes has proven challenging (cf. [52]). Perhaps progress can be made using a large-dimension limit of (bulk) general relativity [53,54], to construct higher-dimensional static braneworld black holes, as done for evaporating black holes [55].

ACKNOWLEDGMENTS

We are grateful to Roberto Emparan, Robie Hennigar, Clifford Johnson, Jorge Rocha and Marija Tomašević for useful discussions and correspondence. A. M. F. is supported by AGAUR Grant No. 2017-SGR 754, and State Research Agency of MICINN through the "Unit of Excellence María de Maeztu 2020-2023" award to the Institute of Cosmos Sciences (CEX2019-000918-M). J. F. P. is supported by the "Atracción de Talento" program Grant No. 2020-T1/TIC-20495 and by the Spanish Research Agency through the Grants No. CEX2020-001007-S and No. PID2021-123017NB-I00, funded by MCIN/AEI/10.13039/501100011033 and by ERDF A way of making Europe. A. S. is supported by STFC Grant No. ST/X000753/1 and was partially supported by the Simons Foundation via *It from Qubit Collaboration* and EPSRC as this work was being completed. M. R. V. is supported by SNF Postdoc Mobility Grant No. P500PT-206877 "Semi-classical thermodynamics of black holes and the information paradox".

[1] S. W. Hawking and D. N. Page, Commun. Math. Phys. **87**, 577 (1983).
[2] J. M. Maldacena and A. Strominger, J. High Energy Phys. 12 (1998) 005.
[3] S. Mano, Mod. Phys. Lett. A **14**, 1961 (1999).
[4] D. Birmingham, I. Sachs, and S. N. Solodukhin, Phys. Rev. D **67**, 104026 (2003).
[5] Y. Kurita and M.-a. Sakagami, Prog. Theor. Phys. **113**, 1193 (2005).
[6] M. Banados, C. Teitelboim, and J. Zanelli, Phys. Rev. Lett. **69**, 1849 (1992).
[7] M. Banados, M. Henneaux, C. Teitelboim, and J. Zanelli, Phys. Rev. D **48**, 1506 (1993); **88**, 069902(E) (2013).
[8] A. Chamblin, R. Emparan, C. V. Johnson, and R. C. Myers, Phys. Rev. D **60**, 064018 (1999).
[9] A. Chamblin, R. Emparan, C. V. Johnson, and R. C. Myers, Phys. Rev. D **60**, 104026 (1999).
[10] M. M. Caldarelli, G. Cognola, and D. Klemm, Classical Quantum Gravity **17**, 399 (2000).
[11] D. Kubiznak and R. B. Mann, J. High Energy Phys. 07 (2012) 033.
[12] S. Gunasekaran, R. B. Mann, and D. Kubiznak, J. High Energy Phys. 11 (2012) 110.
[13] N. Altamirano, D. Kubiznak, and R. B. Mann, Phys. Rev. D **88**, 101502 (2013).
[14] M. B. Ahmed, W. Cong, D. Kubiznak, R. B. Mann, and M. R. Visser, J. High Energy Phys. 08 (2023) 142.
[15] A. M. Frassino, D. Kubiznak, R. B. Mann, and F. Simovic, J. High Energy Phys. 09 (2014) 080.
[16] T. Narayanan and A. Kumar, Phys. Rep. **249**, 135 (1994).
[17] S. de Haro, K. Skenderis, and S. N. Solodukhin, Classical Quantum Gravity **18**, 3171 (2001).
[18] S. de Haro, S. N. Solodukhin, and K. Skenderis, Commun. Math. Phys. **217**, 595 (2001).
[19] R. Emparan, A. Fabbri, and N. Kaloper, J. High Energy Phys. 08 (2002) 043.
[20] R. Emparan, A. M. Frassino, and B. Way, J. High Energy Phys. 11 (2020) 137.
[21] A. Karch and L. Randall, J. High Energy Phys. 05 (2001) 008.
[22] R. Emparan, G. T. Horowitz, and R. C. Myers, J. High Energy Phys. 01 (2000) 007.
[23] R. Emparan, G. T. Horowitz, and R. C. Myers, J. High Energy Phys. 01 (2000) 021.
[24] M. Appels, R. Gregory, and D. Kubiznak, Phys. Rev. Lett. **117**, 131303 (2016).
[25] H. Kudoh and Y. Kurita, Phys. Rev. D **70**, 084029 (2004).
[26] A. Anabalón, M. Appels, R. Gregory, D. Kubizňák, R. B. Mann, and A. Ovgün, Phys. Rev. D **98**, 104038 (2018).
[27] R. Emparan, J. High Energy Phys. 06 (2006) 012.

[28] J. F. Pedraza, A. Svesko, W. Sybesma, and M. R. Visser, J. High Energy Phys. 12 (2021) 134.
[29] A. Svesko, E. Verheijden, E. P. Verlinde, and M. R. Visser, J. High Energy Phys. 08 (2022) 075.
[30] A. M. Frassino, J. F. Pedraza, A. Svesko, and M. R. Visser, Phys. Rev. Lett. **130**, 161501 (2023).
[31] A. M. Frassino, R. B. Mann, and J. R. Mureika, Phys. Rev. D **92**, 124069 (2015).
[32] A. M. Frassino, R. B. Mann, and J. R. Mureika, J. High Energy Phys. 11 (2019) 112.
[33] D. Kastor, S. Ray, and J. Traschen, Classical Quantum Gravity **26**, 195011 (2009).
[34] Our three branches do not coincide with branches $1a$, $1b$, and 2 characterizing the mass in [20]. Precisely, let z_1 be the positive root to $4z^3\nu + 3z^2 - 1 = 0$, z_2 be the positive root of $\nu z^3 + 3z^2 - 3\nu z - 1 = 0$, and $z_3 = \nu^{-1/3}$ (these coincide with [25] upon $z \to \nu z$ and $\lambda = \nu^2$). The value z_1 denotes where the mass has a maximum $M = 1/24\mathcal{G}_3$, and $M = 0$ at z_3. The heat capacity (17) diverges at z_2 and z_3, and is zero at z_1. For any ν there are two branches of positive mass black holes with $\kappa = -1$: branch 2, where $0 < z < z_1$, or $\sqrt{3} < x_1 < \infty$, and branch $1b$, where $z_1 < z < z_3$, or $0 < x_1 < \sqrt{3}$. For $\nu \neq 0$ there is also one branch of negative mass black holes with $\kappa = +1$: branch $1a$, where $z_3 < z < \infty$, or $0 < x_1 < 1$. We can compare to our branches by identifying $z_2 = z_{\min}$ and $z_3 = z_{\max}$ for $\nu > 1$, and $z_2 = z_{\max}$ and $z_3 = z_{\min}$ for $\nu < 1$. Thus, our three branches characterizing $T(z)$ are distinguished by $z_{\min}$ and $z_{\max}$, whereas the three branches of $M(z)$ in [20] are separated by z_1 and z_3.
[35] L. Susskind and J. Uglum, Phys. Rev. D **50**, 2700 (1994).
[36] A. R. Steif, Phys. Rev. D **49**, 585 (1994).
[37] M. Casals, A. Fabbri, C. Martínez, and J. Zanelli, Phys. Lett. B **760**, 244 (2016).
[38] M. Casals, A. Fabbri, C. Martínez, and J. Zanelli, Phys. Rev. D **99**, 104023 (2019).
[39] E. Witten, Adv. Theor. Math. Phys. **2**, 505 (1998).
[40] M. Kord Zangeneh, A. Dehyadegari, A. Sheykhi, and R. B. Mann, Phys. Rev. D **97**, 084054 (2018).
[41] T. Takayanagi, Phys. Rev. Lett. **107**, 101602 (2011).
[42] M. Fujita, T. Takayanagi, and E. Tonni, J. High Energy Phys. 11 (2011) 043.
[43] C. V. Johnson and R. Nazario, arXiv:2310.12212.
[44] C. V. Johnson, Mod. Phys. Lett. A **35**, 2050098 (2020).
[45] R. A. Hennigar, D. Kubizňák, and R. B. Mann, Phys. Rev. Lett. **115**, 031101 (2015).
[46] C. V. Johnson, V. L. Martin, and A. Svesko, Phys. Rev. D **101**, 086006 (2020).
[47] M. Cvetic, G. W. Gibbons, D. Kubiznak, and C. N. Pope, Phys. Rev. D **84**, 024037 (2011).
[48] M. Amo, A. M. Frassino, and R. A. Hennigar, Phys. Rev. Lett. **131**, 241401 (2023).
[49] A. Climent, R. Emparan, and R. A. Hennigar, arXiv:2404.15148.
[50] R. Emparan, J. F. Pedraza, A. Svesko, M. Tomašević, and M. R. Visser, J. High Energy Phys. 11 (2022) 073.
[51] E. Panella and A. Svesko, J. High Energy Phys. 06 (2023) 127.
[52] N. Tanahashi and T. Tanaka, Prog. Theor. Phys. Suppl. **189**, 227 (2011).
[53] R. Emparan, R. Suzuki, and K. Tanabe, J. High Energy Phys. 06 (2013) 009.
[54] R. Emparan and C. P. Herzog, Rev. Mod. Phys. **92**, 045005 (2020).
[55] R. Emparan, R. Luna, R. Suzuki, M. Tomašević, and B. Way, J. High Energy Phys. 05 (2023) 182.